Annals of Operations Research
https://doi.org/10.1007/s10479-022-04923-w

ORIGINAL RESEARCH

Stochastic tramp ship routing with speed optimization: analyzing the impact of the Northern Sea Route on CO_2 emissions

Mingyu Li[1] · **Kjetil Fagerholt**[1] · **Peter Schütz**[1]

Accepted: 2 August 2022

Abstract
To address the decarbonization challenge, we consider a tramp ship routing problem with speed optimization where the availability of future cargoes is uncertain. We propose a two-stage stochastic programming model to solve it. The first stage of the model decides on the deterministic cargoes with the known availability, while the second stage decides on the detailed routing and scheduling plans with the available spot cargoes revealed. Since sailing speed heavily influences on the fuel consumption, and hence costs and emissions, we include the ships' speeds along the different sailing legs as decision variables. The opening of the Northern Sea Route (NSR) provides a shorter alternative in connecting Asia and Europe, which may benefit the shipping industry in reducing CO_2 emissions. We use our model to evaluate the impact of NSR on CO_2 emissions in tramp shipping considering speed optimization and possible future carbon tax schemes, such as fixed and progressive carbon taxes. The computational results indicate that using the NSR improves the gross margins and reduces the CO_2 emissions for tramp operators.

Keywords Stochastic tramp ship routing and scheduling problem · Speed optimization · Northern Sea Route · CO_2 emissions

1 Introduction

The shipping industry has committed to the goal set by International Maritime Organization (IMO) to reduce CO_2 emissions by 40% by 2030 compared to the baseline in 2008 to contribute to combating climate change. However, from 2012 to 2018, the emissions from global shipping have been constantly increasing (International Maritime Organization, 2020). Actions have to be taken to achieve the decarbonization goal.

Speed optimization and carbon tax are among the candidate measures to cope with the decarbonization challenge. There is a linear relationship between the fuel consumption and

✉ Mingyu Li
mingyu.li@ntnu.no

[1] Department of Industrial Economics and Technology Management, Norwegian University of Science and Technology, Trondheim, Norway

Published online: 24 August 2022

CO_2 emissions. The fuel consumption rate is vessel-specific, strongly influenced by speed (Andersson et al., 2015), but depends also on the ship's loading status (loaded or in ballast) as well as the sailing environments. More specifically, the relationship between the fuel consumption rate per time unit and speed can usually be approximated by a cubic function (Ronen, 1982), and hence, the fuel consumption per distance unit becomes a quadratic function of speed. In this paper we use fuel consumption per distance on rate. With speed optimization or speed reduction, vessels operate at a speed which is lower than the design speed to reduce fuel consumption and consequently CO_2 emissions. In practice, operating at a slower speed, referred to as slow steaming, has been prevailing in the shipping industry for fuel consumption reduction.

According to Zhang and Baranzini (2004), carbon tax is an excise tax imposed based on the carbon content of fossil fuels, which incentivizes the shipping industry to reduce CO_2 emissions. The European Union Emissions Trading System (EU ETS), which functions in a similar way to carbon tax, has been implemented since 2005 and has proven to be effective in reducing CO_2 emissions. The total emissions capacity is distributed among the member countries as allowances, each unit of which corresponds to a unit CO_2 emission. When a member country emits more than its allowance, it has to purchase allowance from other countries that may have remaining allowance to gain economic rewards. Therefore, the ETS can be translated to an extra cost on each unit of CO_2 emissions, which is similar to imposing a per unit carbon tax.

In addition to speed optimization and carbon tax, using alternative maritime routes such as the Northern Sea Route (NSR) offers a new option for decarbonization. The sea ice extent in the Arctic has retreated to record low in recent years, leading to the opening of NSR as a shorter maritime route alternative in connecting Asia and Europe. Compared to the traditional Suez Canal Route (SCR), sailing through the NSR may save 42% distance (Schøyen & Bråthen, 2011). This reduced sailing distance may benefit the operator in reducing fuel consumption and CO_2 emissions. However, the sea ice along the NSR limits the sailing speed and requires additional support for example from ice breaking vessels. The evaluation of the impact of introducing the NSR into maritime transportation is hence complicated by the trade-off between the shorter distance of using NSR and the faster speed along the SCR.

Tramp shipping is the major transportation mode for bulk cargoes including oil and gas which comprise over 75% cargo volumes in international maritime trade in 2019 (United Nations Conference on Trade and Development, 2020). A reduction in CO_2 emissions in tramp shipping therefore plays an important role in decarbonization for the whole shipping industry. In tramp shipping, the operations of the fleet follows available cargoes, similar to taxis serving passengers. The operations include accepting and transporting available cargoes to maximize the total profits. However, which cargoes will be available during the planning horizon is uncertain when the operations of the tramp fleet are planned. Some available cargoes are known in advance, and the operator may choose to enter into long-term agreements referred to as Contracts of Affreightment (CoAs) (Vilhelmsen et al., 2015). A CoA usually specifies a series of cargoes with some information about cargo quantities and time-wise spread of them. The decisions about which contract cargoes to accept are hence also made on a tactical level in advance of the operations. The operator will honor the contract cargo commitments during the operational planning of the fleet. As a complement to the contract cargoes, available spot cargoes can be accepted to fill in the remaining time slots to improve the utilization of the fleet on the operational level (Christiansen et al., 2007). This Tramp Ship Routing and Scheduling Problems (TSRSPs) with uncertain cargo availability is characterized by the sequential determination of acceptance of cargoes: the acceptance and

schedule of contract cargoes are on the tactical level while the acceptance of the spot cargoes along with the detailed routes and schedules fall onto the operational level.

We formulate our research questions as follows in order to address the objectives of this study. What is the impact of the NSR on CO_2 emissions in tramp shipping? We develop further sub-question for the purposes of this study: does this impact change when allowing speed optimization and imposing carbon tax? In order to carry out the analysis, we propose a two-stage stochastic programming model for the stochastic TSRSP with speed optimization under carbon tax. The model maximizes the gross margin from transporting cargoes with possible carbon tax included in the costs. The model allows using the NSR as an alternative to the SCR. Therefore, we compare the results with and without using the NSR to evaluate its impact.

We summarize our contributions as follows: In terms of modeling, we extend the TSRSP with uncertain cargoes in Li et al. (2020) to include carbon tax and speed optimization, where we model the speed with a linearized approximation. Our model allows speed optimization for each voyage and is able to capture different fuel consumption rates for different loading status and on different routes. As for solution methods, we solve the problem with Sample Average Approximation (SAA). We also propose effective pre-processing procedures and valid inequalities to speed up the solution process. On evaluating the impact of NSR, we include the impact on reducing CO_2 emissions, where we allow speed optimization and consider possible carbon tax schemes on fleet level.

We arrange the remainder of this paper as follows. Relevant literature are reviewed in Sect. 2. We describe the problem of the optimization model in Sect. 3. Section 4 presents our modeling approaches, followed by the model formulation. In Sect. 5 we discuss the procedures applied to speed up solution process. We introduce the input data and scenario tree generation in Sect. 6. Section 7 discusses the results of our case study, ending with conclusions in Sect. 8.

2 Relevant literature

In this section, we review the literature on the effect on CO_2 emissions of introducing NSR. In addition, we review the literature on stochastic TSRSPs, TSRSPs with speed optimization and TSRSPs addressing CO_2 emissions.

Much research has been devoted to investigating the economic or navigational feasibility of the NSR, of which more comprehensive and up-to-date reviews can be found in Milaković et al. (2018), Theocharis et al. (2018) and Meng et al. (2017). Among the 33 papers reviewed in Theocharis et al. (2018), only three of them account for both cost and CO_2 emissions in assessing the feasibility of NSR for tramp shipping, and the evaluation in all three papers is established upon a single voyage basis. Schøyen and Bråthen (2011) base their comparison on the equivalent speeds which refer to the speeds needed to sail between two given ports via the SCR and NSR with the same duration. They calculate the total costs and CO_2 emissions at the equivalent speeds for a single voyage. Zhao and Hu (2016) compare the total costs and greenhouse gas emissions for a voyage via SCR and NSR based on the voyage of Yongsheng where they consider the average speed along the SCR and NSR to be the same. Similar to Schøyen and Bråthen (2011), Pierre and Olivier (2015) compare the daily average costs including a price for CO_2 emissions via the SCR and NSR at a range of equivalent speeds. They optimize the operational speed along the SCR for a single voyage taking market conditions such as freight rate and fuel price into account. They evaluate the costs along the

SCR at the optimized speeds and the costs along the NSR at the equivalent speed. All three papers agree upon that using the NSR is beneficial to CO_2 emissions reduction. However, their conclusions diverge when it comes to the economic performances. Both Zhao and Hu (2016) and Schøyen and Bråthen (2011) conclude that because of the shorter distance, the estimated total single voyage costs for the NSR are lower than the SCR. Meanwhile, Pierre and Olivier (2015) argue that affected by the low spot freight rate, vessels operate at a lowest level speed on SCR, with a low fuel consumption. Thus the fuel savings of using the NSR is becoming less attractive. They further impose a CO_2 tax at different rates. Their computational study show that only when the carbon tax is as high as 100 USD per ton CO_2 emissions, using NSR brings significant savings. In reality, the operational speeds of ship are not necessarily optimized on a single voyage level, but the fleet operations level.

Even though the occurrence of future cargoes is stochastic by nature, uncertain cargoes have not received much attention in literature on tramp shipping. Li et al. (2020) is an exception. Li et al. (2020) address TSRSPs with uncertain cargo availability and propose a two stage stochastic programming model formulation. In the model, they introduce routing flexibility for using the NSR as an alternative to the SCR into the TSRSP. With the proposed model, they analyze the impact of introducing the NSR into tramp shipping on a fleet operation level by comparing the results with and without the NSR allowed in the model.

The majority of existing work that handles the availability of cargoes as uncertain are in industrial shipping, which is similar to tramp shipping in operational characteristics. The main difference is that in industrial shipping, the operator owns both the fleet and the cargoes, aiming to minimize the cost for transporting all cargoes. From an operations research point of view, the typical Industrial Shipping Routing and Scheduling Problems (ISRSPs) can be treated as a special case of TSRSP, where no spot cargoes are present and all contract cargoes are accepted (Christiansen & Fagerholt, 2014). Tirado et al. (2013) present an ISRSP where new contract cargoes arrive randomly and constantly throughout the planning horizon. Accordingly the decisions are replanned every time a new cargo appears. Wu et al. (2018) include the option to transport spot cargoes when the vessel is repositioning back to the original port after the contract cargo is delivered. However, none of the above mentioned research look into speed optimization or CO_2 emissions. Nor do they consider the use of the NSR.

Speed optimization has been addressed in deterministic TSRSPs where cargoes are assumed to be known at the time of planning. As fuel costs constitute a large proportion of operational costs in shipping, research has been motivated to include speed optimization into TSRSP for the economic benefits in reducing the fuel cost. Speed optimization is usually modeled using either linear model with discretized speeds (Castillo-Villar et al., 2014; Wen et al., 2016), or non-linear model with continuous speeds (Norstad et al., 2011; Yu et al., 2019). The introduction of speed optimization into the TSRSP increases the complexity of the problem, which is reflected by that all the aforementioned papers unanimously resort to heuristic methods for efficient solutions.

In addition to the economic benefits, speed optimization can bring environmental benefits such as reduction in CO_2 emissions. The increasing social awareness in reducing CO_2 emissions in recent years is reflected in the literature with discussion on the environmental implications of speed optimization. Wang et al. (2019) investigate the effect of policies such as carbon tax and emissions trading system for reducing CO_2 emissions with their proposed model for a TSRSP with speed optimization. Their computational study demonstrates that the operators slow down the vessels and emit less CO_2 in response to the elevated fuel price resulting from the policies. It is worth mentioning that Wen et al. (2017) address the general emissions in a ship routing and speed optimization problem which can be applied in both

liner and tramp shipping. Since emissions are directly proportional to fuel consumption, they use fuel consumption as objective function to be minimized. They emphasize the importance of addressing the loading status when considering the fuel consumption as sailing in ballast at a higher speed may still generate less emissions than sailing fully loaded at a lower speed. However, both of the aforementioned studies consider neither the effect of alternative routes in reducing CO_2 emissions nor uncertain spot cargoes.

To the best of our knowledge, speed optimization for entire fleet and the introduction of carbon tax have not been addressed when evaluating the impact of the NSR. Our paper extends the existing literature in these respects. By including fleet-level speed optimization and carbon tax into the evaluation of NSR, we explore the potential of using NSR in reducing CO_2 emissions in more detail. Besides, we present a new formulation of stochastic TSRSP including speed optimization and routing flexibility under carbon tax. We show in addition how to improve the model performance.

3 Problem description

We present a stochastic TSRSP with speed optimization and routing flexibility under carbon tax. A tramp operator plans its fleet operations in two stages: In the first stage, the tramp operator knows which cargoes are currently available in the market (i.e. the deterministic cargoes). At this point in time, the operator also has information regarding uncertain spot cargoes, i.e. cargoes that might or might not become available in the future (the stochastic cargoes). The operator then decides which of the deterministic cargoes to accept, which vessel to allocate each accepted cargo to and when to pickup these cargoes. In the second stage, the tramp operator gets to know which of the uncertain spot cargoes are available in the market. The operator then chooses which spot cargoes to accept and decides the detailed operational plan of the fleet given the first stage decisions. We assume that the deterministic cargoes have already been made available to the operator e.g., through ship brokers or shippers. For the uncertain cargoes we assume that the tramp operator can use own experience and historical data indicating typical loading and unloading ports for relevant cargoes.

Since we want to study the effect of using the NSR, we assume that the candidate cargoes are to be transported within and between Asia and Europe. The revenue for each cargo is specified. Once a cargo is accepted, it has to be picked up within a specific pickup time window. Based on the regions involved to transport a cargo, we divide them into local cargoes, where both ports are either in Asia or Europe, and intercontinental cargoes, where one port is in Asia and the other is in Europe. A voyage involves sailing from one port to another. Then the concept of local and intercontinental cargoes extends to *local voyages* and *intercontinental voyages*. For intercontinental voyages, it is possible to choose sailing through either the SCR or the NSR, introducing routing flexibility, as illustrated in Fig. 1, see also Li et al. (2020). We consider the cargo size to be equal to the loading capacity of a vessel. According to the loading status of a vessel, we divide the voyages into *delivery voyages* sailing fully loaded when transporting a cargo, and *repositioning voyages* sailing in ballast between transporting two consecutive cargoes.

The ship operator controls a heterogeneous fleet of vessels, where the vessels have different fuel consumption profiles and are located at different initial positions at the beginning of the planning horizon. The fuel consumption profile describes the fuel consumption rate of a specific vessel at given speeds, which is affected by the loading status and the sailing route. Decisions on the vessels' speeds have to be made for every voyage, regardless delivery or

Fig. 1 Illustration of routing flexibility (Li et al., 2020)

repositioning. Using a higher speed may allow the vessel to transport more cargoes, while using a slower speed may reduce fuel consumption and hence CO_2 emissions. The trade-off between sailing time and costs has to be taken into consideration when deciding the speeds.

We include the voyage costs and idle costs for each vessel in the fleet and the carbon tax for the whole fleet within the planning horizon. The voyage costs consist of port dues and fuel costs, which apply to both delivery voyages and repositioning voyages. For intercontinental voyages, canal fees for the SCR and ice-breaking support fees for the NSR will occur. In additions, due to the presence of sea ice, the operational speeds along the NSR are limited. When a vessel is neither sailing a delivery voyage or a repositioning voyage, it still consumes fuel, though at a much slower rate. We consider this fuel cost to be the idle cost of a vessel. To meet the pickup time window of a cargo, vessels may arrive early at port and wait, but the waiting time is considered as being idle. The carbon tax is levied on the carbon content of the total fuel consumed by the entire fleet over the planning horizon. The total CO_2 emissions are estimated based on both the voyage-related fuel consumption and the idle fuel consumption for each individual vessel. The carbon tax can either follow a flat or progressive tax scheme. In the flat tax scheme, the tax is directly proportional to the total CO_2 emissions (and hence the fuel consumption), while in the progressive tax scheme, the tax per unit of CO_2 emitted increases progressively.

The objective is to maximize the expected gross margin, which is calculated as the total revenues from transporting the cargoes minus the variable sailing costs, consisting of fuel costs, canal fees, port costs, ice-breaking support fees and carbon tax. In the first stage the operator decides on the acceptance of the deterministic cargoes, and for each accepted cargo, the corresponding vessel as well as time to pick it up. With the available spot cargoes revealed in the second stage, the operator decides on which of those to accept, the sequence of transporting the accepted cargoes for each vessel, whether to sail through the NSR or the SCR for intercontinental voyages, the speeds for every delivery or repositioning voyage and consequently pickup times of all cargoes.

4 Model formulation

Before presenting our two-stage stochastic programming model, we explain the modeling approach and introduce the notation.

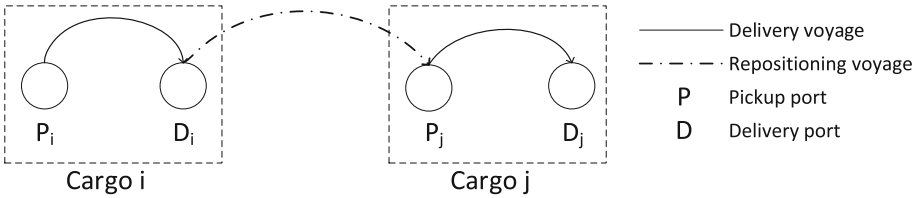

Fig. 2 Illustration of voyages between transporting two cargoes (Li et al., 2020)

4.1 Modeling approach

Cargo-based voyages

We model the routing decisions of a vessel similar to Vilhelmsen et al. (2015) by the sequence of cargoes transported based on the assumption that the cargo size equals a full shipload. Figure 2 illustrates the voyages when cargo j is the next subsequent cargo following cargo i. The vessel first loads cargo i from port P_i, sails loaded to port D_i to deliver cargo i. Then the vessel repositions to port P_j to pick up cargo j and continues to D_j to unload cargo j. Transporting cargoes i and j sequentially implies visiting a sequence of ports in the order of $P_i \rightarrow D_i \rightarrow P_j \rightarrow D_j$.

Cargoes

We model routing flexibility (i.e. whether to use the SCR or the NSR) for delivery voyages through cargo duplication. In each scenario, we have a total of at most N cargoes available, divided into N^I intercontinental and N^L local cargoes. Each of the intercontinental cargoes is duplicated into a cargo i transported via the SCR (SCR cargo) and a corresponding NSR cargo $i+N$, and the sailing times, costs as well as CO_2 emissions are calculated accordingly. However, the duplicated cargo pair shares the same revenue and pickup time windows.

To initialize the problem, we create an origin node for each vessel, i.e. an artificial cargo without revenue or costs, that represents the port at which the vessel becomes available. Similarly, we introduce an artificial destination node for each vessel, also represented by an artificial cargo without revenue or costs, which allows us to control the port a vessel ends up in at the end of the planning horizon. By adjusting the repositioning times and costs between the origin/destination node and the other available cargoes, we are able to model different initial and final locations as well as the time when a vessel becomes available. The available cargoes, together with the artificial origin and destination cargoes form an extended cargo set $\mathcal{C}_s^E$.

Modeling speed-fuel consumption curve

The operational speed of a given vessel is usually within a certain range. A minimum speed has to be maintained for safety and economical concerns. Meanwhile, limited by the machinery of the speed and sailing environment, there is a corresponding a maximum speed. According to Ronen (1982), within this speed range, the fuel consumption per distance can usually be approximated as a quadratic and convex function over speed. Such non-linearity is undesirable in modeling due to the extra computational burden coming along. To avoid this issue, we follow the linear approximation introduced in Andersson et al. (2015).

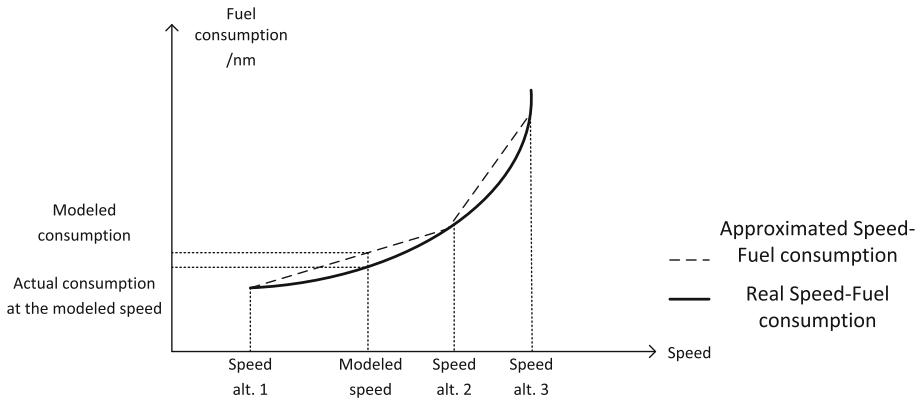

Fig. 3 Illustration of speed-fuel consumption approximation

We use a piecewise linear function with three breakpoints to approximate the speed fuel consumption curve, see Fig. 3. In the figure, speed alternatives 1, 2 and 3 correspond to minimum speed, design speed and maximum speed, respectively. Let S_i be the sailing speed and w_i be the weight of speed alternative i. Any speed S can then be modeled as a convex linear combination of speeds, i.e. $S = \sum_i w_i \cdot S_i$ given that $\sum_i w_i = 1$. Due to the convexity of the fuel consumption function, an optimal solution will always be a linear combination of two neighboring speed points. Modeled Speed in Fig. 3 can therefore be represented as $w_1 \cdot S_1 + (1 - w_1) \cdot S_2$ (as $w_1 + w_2 = 1$).

Let T_i be the sailing time associated with speed alternative i. We then approximate sailing time by a linear combination of sailing times using the same weights, i.e. $w_1 \cdot T_1 + (1 - w_1) \cdot T_2$, for the Modeled Speed in Fig. 3. The corresponding fuel consumption is estimated in the same manner, again using the same weights. Fuel consumption is then converted to CO_2 emissions using an emission factor. Andersson et al. (2015) show that the error introduced by the piecewise linearization overestimates both fuel consumption and sailing time. However, as the error is usually small and far below the uncertainty in other parameters, we consider this approach to be appropriate for our purposes.

Carbon tax

CO_2 emissions are taxed on a fleet level, not on a voyage or ship level. We model a progressive carbon tax, as shown in Fig. 4a. In a progressive tax scheme, the CO_2 emissions is divided into several levels. As the emissions reaches a higher level, a higher tax rate applies. Similar to the modeling of the fuel consumption versus speed, the model will always automatically allocate the emissions first to the level with the least tax rate, since the tax is lower, until no more emissions allowed at this level. In addition to progressive tax scheme, a flat tax scheme is also common where a constant tax rate apply to emissions at any level, illustrated in Fig. 4b. The flat tax scheme can be seen as a special case of the progressive tax, where the first emissions level is set to a sufficiently high amount.

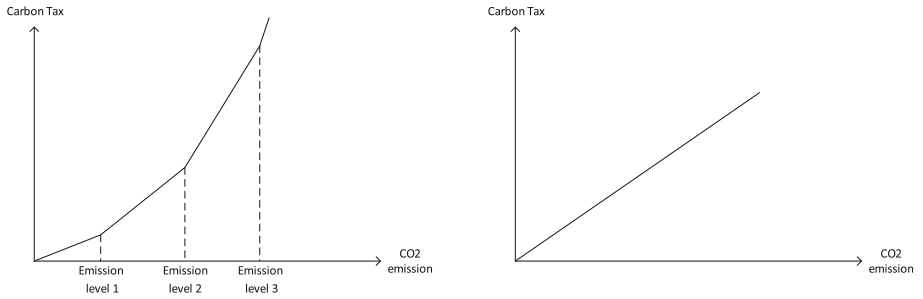

(a) Illustration of a progressive carbon tax **(b)** Illustration of a flat carbon tax

Fig. 4 Illustration of different tax schemes

4.2 Notation

We introduce the following notation:

Sets

$\mathcal{G}_s^E$	Extended set of available cargoes, including the duplicated intercontinental cargoes, the artificial origin and destination cargoes in scenario s
$\mathcal{G}^D$	Set of deterministic cargoes
$\mathcal{G}_s^I$	Set of available intercontinental cargoes in scenario s
$\mathcal{G}_s^L$	Set of available local cargoes in scenario s
$\mathcal{G}^U$	Set of uncertain spot cargoes
$\mathcal{K}$	Set of speeds
$\mathcal{L}$	Set of CO_2 emissions levels
$\mathcal{R}$	Set of routes
$\mathcal{S}$	Set of scenarios
$\mathcal{V}$	Set of vessels

Indices

i, j	Cargo index
k	Speed index
l	CO_2 emissions tax level index
r	Route index
s	Scenario index
v	Vessel index

Parameters

A_{is}	Earliest pickup time for cargo i in scenario s
B_{is}	Latest pickup time for cargo i in scenario s
C_v^F	Daily idle cost for vessel v
C_{vijrsk}^R	Repositioning cost for vessel v between transporting cargo i and j via route r in scenario s at speed k

C_l	Unit carbon tax at emission level l
C_{visk}	Delivery cost for transporting cargo i with vessel v in scenario s at speed k
E_v	An artificial destination cargo for vessel v
H	Length of planning horizon
M_v^F	Daily idle CO_2 emissions for vessel v
M_{vijrsk}^R	CO_2 emissions for a repositioning voyage for vessel v between transporting cargo i and j via route r in scenario s at speed k
M_{visk}	CO_2 emissions for transporting cargo i with vessel v in scenario s at speed k
N	Number of cargoes
O_v	An artificial origin cargo for vessel v
P_s	Probability of scenario s
Q_l	Maximum CO_2 emissions at level l
R_{is}	Revenue of transporting cargo i in scenario s
T_{vijrsk}^R	Sailing time for a repositioning voyage for vessel v between transporting cargo i and j via route r in scenario s at speed k
T_{visk}	Sailing time for transporting cargo i with vessel v in scenario s at speed k

Decision variables

f_{ls}	CO_2 emissions at level l in scenario s
n_{vi}	1 if vessel v is assigned to transport deterministic cargo i, 0 otherwise
t_{vi}	The planned pickup time of a deterministic cargo i by vessel v
τ_{vis}	The planned pickup time of a cargo i by vessel v in scenario s
w_{vijrsk}	The weight of speed alternative k for the sailing with vessel v delivering cargo i, repositioning via route r then directly picking up cargo j in scenario s
x_{vijrs}	1 if vessel v delivers cargo i, repositions via route r then directly picks up cargo j in scenario s, 0 otherwise
y_{visk}	The weight of speed alternative k for the sailing with vessel v delivering cargo i in scenario s

4.3 Model

With the notation introduced above we present the formulation of the two-stage stochastic TSRSP with speed optimization and routing flexibility.

$$\max \sum_{s\in\mathcal{S}} P_s \left\{ \sum_{v\in\mathcal{V}} \sum_{i\in\mathcal{G}_s^E} \sum_{k\in\mathcal{K}} (R_{is} y_{visk} - C_{visk} y_{visk} - \sum_{j\in\mathcal{G}_s^E} \sum_{r\in\mathcal{R}} C_{vijrsk}^R w_{vijrsk}) \right.$$
$$\left. - \sum_{v\in\mathcal{V}} C_v^F (H - \sum_{i\in\mathcal{G}_s^E} \sum_{k\in\mathcal{K}} (T_{visk} y_{visk} + \sum_{j\in\mathcal{G}_s^E} \sum_{r\in\mathcal{R}} T_{vijrsk}^R w_{vijrsk})) - \sum_{l\in\mathcal{L}} C_l f_{ls} \right\} \quad (1)$$

subject to

$$\sum_{v\in\mathcal{V}} n_{vi} \le 1 \qquad i \in \mathcal{G}^D, \quad (2)$$

$$\sum_{j\in\mathcal{G}_s^E} \sum_{r\in\mathcal{R}} (x_{vijrs} + x_{v,i+N,jrs}) = n_{vi} \qquad v \in \mathcal{V}, i \in \mathcal{G}^D \cap \mathcal{G}_s^I, s \in \mathcal{S}, \quad (3)$$

$$\sum_{j\in\mathcal{G}_s^E}\sum_{r\in\mathcal{R}} x_{vijrs} = n_{vi} \qquad v\in\mathcal{V}, i\in\mathcal{G}^D\cap\mathcal{G}_s^L, s\in\mathcal{S}, \tag{4}$$

$$\tau_{v,i+N,s} = t_{vi} \qquad v\in\mathcal{V}, i\in\mathcal{G}^D\cap\mathcal{G}_s^I, s\in\mathcal{S}, \tag{5}$$

$$\tau_{vis} = t_{vi} \qquad v\in\mathcal{V}, i\in\mathcal{G}^D, s\in\mathcal{S}, \tag{6}$$

$$\sum_{j\in\mathcal{G}_s^E}\sum_{r\in\mathcal{R}} (x_{vijrs} + x_{v,i+N,jrs}) \le 1 \qquad i\in\mathcal{G}^U\cap\mathcal{G}_s^I, s\in\mathcal{S}, \tag{7}$$

$$\sum_{j\in\mathcal{G}_s^E}\sum_{r\in\mathcal{R}} x_{vijrs} \le 1 \qquad i\in\mathcal{G}^U\cap\mathcal{G}_s^L, s\in\mathcal{S}, \tag{8}$$

$$\sum_{j\in\mathcal{G}_s^E}\sum_{r\in\mathcal{R}} x_{v,O_v,jrs} = 1 \qquad v\in\mathcal{V}, s\in\mathcal{S}, \tag{9}$$

$$\sum_{i\in\mathcal{G}_s^E}\sum_{r\in\mathcal{R}} x_{vi,E_v,rs} = 1 \qquad v\in\mathcal{V}, s\in\mathcal{S}, \tag{10}$$

$$\sum_{i\in\mathcal{G}_s^E}\sum_{r\in\mathcal{R}} x_{vijrs} - \sum_{i\in\mathcal{G}_s^E}\sum_{r\in\mathcal{R}} x_{vjirs} = 0$$
$$v\in\mathcal{V}, j\in\mathcal{G}_s^E\setminus\{O_v, E_v | v\in\mathcal{V}\}, s\in\mathcal{S}, \tag{11}$$

$$\sum_{k\in\mathcal{K}} y_{visk} = \sum_{j\in\mathcal{G}_s^E}\sum_{r\in\mathcal{R}} x_{vijrs}$$
$$v\in\mathcal{V}, i\in\mathcal{G}_s^E\setminus\{O_v, E_v | v\in\mathcal{V}\}, s\in\mathcal{S}, \tag{12}$$

$$\sum_{k\in\mathcal{K}} w_{vijrsk} = x_{vijrs} \qquad v\in\mathcal{V}, i, j\in\mathcal{G}_s^E, r\in\mathcal{R}, s\in\mathcal{S}, \tag{13}$$

$$\sum_{l\in\mathcal{L}} f_{ls} = \sum_{v\in\mathcal{V}} M_v^F (H - \sum_{i\in\mathcal{G}_s^E}\sum_{k\in\mathcal{K}} (T_{visk} y_{visk} + \sum_{j\in\mathcal{G}_s^E}\sum_{r\in\mathcal{R}} T_{vijrsk}^R w_{vijrsk}))$$
$$+ \sum_{v\in\mathcal{V}}\sum_{i\in\mathcal{G}_s^E}\sum_{k\in\mathcal{K}} M_{visk} y_{visk}$$
$$+ \sum_{v\in\mathcal{V}}\sum_{i\in\mathcal{G}_s^E}\sum_{k\in\mathcal{K}}\sum_{j\in\mathcal{G}_s^E}\sum_{r\in\mathcal{R}} M_{vijrsk}^R w_{vijrsk} \qquad s\in\mathcal{S}, \tag{14}$$

$$f_{ls} \le Q_l \qquad l\in\mathcal{L}, s\in\mathcal{S}, \tag{15}$$

$$A_{is} \le \tau_{vis} \le B_{is} \qquad v\in\mathcal{V}, i\in\mathcal{G}_s^E, s\in\mathcal{S}, \tag{16}$$

$$\sum_{k\in\mathcal{K}} (T_{visk} y_{visk} + \sum_{r\in\mathcal{R}} T_{vijrsk}^R w_{vijrsk}) \le$$
$$(B_{is} + T_{vis1} - A_{js})(1 - \sum_{r\in\mathcal{R}} x_{vijrs})$$
$$+\tau_{vjs} - \tau_{vis} \qquad v\in\mathcal{V}, i, j\in\mathcal{G}_s^E, s\in\mathcal{S}, \tag{17}$$

$$f, \tau, t, w, y \ge 0 \tag{18}$$

$$n, x \in \{0, 1\} \tag{19}$$

The objective function (1) maximizes the expected value of gross margin. The first line subtracts the speed-dependent delivery costs and repositioning costs from the total revenues. In the second line, we first calculate the total idle fuel costs for the fleet, based on the idle

time after sailing and repositioning is time deducted from the planning horizon. The last term sums up the total carbon tax.

Constraints (2) state that a deterministic cargo is assigned to at most one vessel. Constraints (3) to (6) are the non-anticipativity constraints. The right-hand-side (RHS) in Constraints (3) and (4) indicates if cargo i is accepted and assigned to vessel v in the first stage ($n_{vi} = 1$). The left-hand-side indicates if a repositioning voyage is planned after delivering cargo i with vessel v for intercontinental cargoes and local cargoes respectively in the second stage. Constraints (3) and (4) also ensure that for each of the accepted deterministic cargoes in the first stage, it has to be transported with the same vessel v in every scenario in the second stage. Meanwhile, if a deterministic cargo is not accepted in the first stage ($n_{vi} = 0$), it can not be transported in the second stage. Similarly, the RHS in constraints (5) and (6) sets the planned pickup time for deterministic cargoes in the first stage. Constraints (5) and (6) stipulate that the pickup time decided in the first stage for each accepted deterministic cargo has to be implemented in all possible scenarios in the second stage. Constraints (7) and (8) determine whether to accept a spot cargo and ensure that at most one vessel will be assigned to an available spot cargo. With Constraints (9) and (10), all vessels begin from the original locations and end in the corresponding destination port at the end of planning horizon. Constraints (11) make sure that for the accepted cargoes, both the pickup ports and delivery ports are visited. Constraints (12) and (13) allow vessels to select speeds for delivery and repositioning voyages respectively by assigning weights to the discrete speed alternatives. Constraints (14) sum up the total idle emissions as well as both delivery voyages and repositioning voyages CO_2 emissions in every scenario and Constraints (15) allocate the correct amount of CO_2 emissions at each tax rate level. Constraints (16) require the planned pickup times follow the pickup time windows. Constraints (17) make sure there is enough time reserved for vessel v to transport cargo i and to reposition for cargo j if cargoes i and j are planned to be transported consecutively with the same vessel. Constraints (18) are the nonnegativity constraints for the continuous variables and Constraints (19) are the binary requirements for the binary variables. Note that indices have been omitted in both.

5 Improving model performance

In the following section, we propose pre-processing procedures and valid inequalities to speed up the solution process. In this section, we use a simplified notation of Sect. 4.2. The simplified notation is in parenthesis when it first appears. Note that scenario index s is omitted throughout this section.

5.1 Incompatible time window elimination

We eliminate the repositioning variables that connect cargoes with incompatible pickup time windows. In order to reposition to cargo j after i, the difference between B_j, the latest pickup time of the cargo j and A_i, the earliest pickup time for cargo i should be long enough. The minimum time required between picking up cargoes i and j is equal to the sum of $T_{vi,|\mathcal{K}|}$ (T_{viK}), delivering cargo i at the maximum speed $|\mathcal{K}|$ (K), and $T^R_{vijr|\mathcal{K}|}$ (T_K^{Repo}), repositioning through route r at the maximum speed K as well. If $B_j - A_i$ is shorter than $T_{viK} + T_K^{Repo}$, it is impossible to transport the two cargoes sequentially with the same vessel. In this case we consider the two time windows are incompatible and the corresponding x variables are

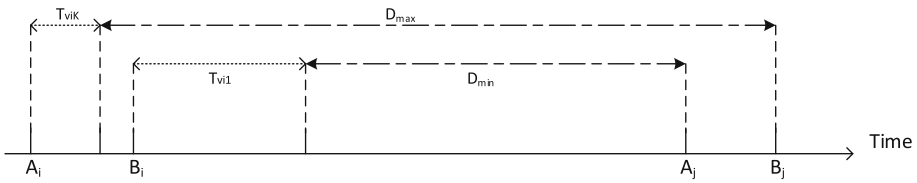

Fig. 5 Illustration of available time range

thus eliminated beforehand. If intercontinental repositioning is involved, we process the two routes separately. Note that it is possible that the pickup time windows are incompatible through NSR but compatible though SCR, or vice versa.

5.2 Repositioning speed variables reduction

We define the duration between transporting cargo i and j (duration) as the time from delivering cargo i to picking up cargo j. This duration includes the repositioning time between i and j, and potentially waiting time. Then the duration between two sequentially transported cargoes is limited by the achievable time range determined by the port distances and speed ranges, as well as the available time range based on the pickup time windows. We reduce repositioning speed variables with these two time ranges.

The achievable time range is straight forward. To reposition between cargo i and j with vessel v, we consider sailing the distance between delivery port for cargo i and pickup port of cargo j at the maximum speed alternative K, corresponding to T_K^{Repo} as the minimum achievable time. Any duration below T_K^{Repo} requires a higher speed which is unachievable by the vessel. Without waiting, the maximum achievable time between i and j correspond to repositioning at the minimum speed alternative 1, leading to T_1^{Repo}. The duration above this T_1^{Repo} is still achievable, however since the speed can not be lowered, the vessel has to wait. We use T_1^{Repo} to decide if waiting is inevitable.

The available time range considers the pickup time windows and the time spent on delivering cargo i, which is illustrated in Fig. 5. The maximum available time D_{max} corresponds to picking up cargo i at the earliest pickup time A_i, after T_{viK} spent delivering cargo i at the maximum speed alternative K and picking up cargo j at the latest pickup time B_j. Similarly the available time D_{min} is determined by picking up cargo i at the latest time B_i, spending T_{vi1} in delivering at the minimum speed alternative 1, cargo j at the earliest pickup time A_j.

The duration between transporting cargo i and j in any feasible solution shall be both achievable to the vessel, and within the available time range. Mathematically, the duration falls into $[D_{min}, D_{max}] \cap \left[T_K^{Repo}, H\right]$ where H is the length of the planning horizon. We address two special cases first.

If $D_{max} \leq T_K^{Repo}$, cargo j will no longer be available after repositioning from cargo i with vessel v. The time windows of the two cargoes are incompatible and eliminated as described in Sect. 5.1.

If $T_{vijrs1}^R \leq D_{min}$, $[D_{min}, D_{max}] \cap \left[T_K^{Repo}, H\right] = [D_{min}, D_{max}]$. Even if sailing at the minimum speed, the vessel will arrive too early at port and has to inevitably wait until the opening of pickup time window for cargo j. In this case, using any speed higher than the minimum speed will lead to a higher fuel cost due to higher fuel consumption rate at a higher speeds. Moreover, using higher speed does not help to pickup cargo j earlier. It means

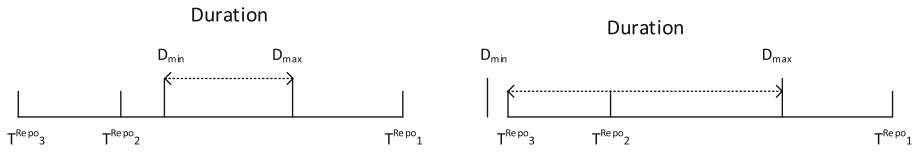

(a) Speed alternative 3 out of the duration **(b)** All speed alternatives are in the duration

Fig. 6 Finding speed alternatives to remove

arriving even earlier at port, waiting longer and hence idle costs increase as well. In case of inevitable waiting, any speed higher than the minimum speed is dominated, and can thus be eliminated.

If none of the above two special cases occur, we use the duration calculated above to eliminate the speed alternatives that will not be included in the optimal solution. Due to the convexity of approximated speed-fuel consumption curve, any speed to model will only be represented by two neighbouring speed alternatives in the optimal solution. We refer the interested reader to Andersson et al. (2015) for a detailed discussion. Figure 6 lists two possibilities for an simplified case where speed alternative 1 corresponds to the minimum speed while speed alternative 3 stands for the maximum speed. In Fig. 6a, the optimal solution will only include the combination of T_2^{Repo} and T_1^{Repo}. Speed 3 will never be present in an optimal solution and the corresponding variable can thus be removed. In contrast, in Fig. 6b, the optimal solution may include a linear combination of T_3^{Repo} and T_2^{Repo}, or T_2^{Repo} and T_1^{Repo}. None of the three speeds can be eliminated.

We skip the eliminated variables during variable generation.

5.3 Dominance in repositioning routing variables

As a result of routing flexibility, each possible intercontinental repositioning yields two variables: through SCR or NSR. To reduce the feasible space of the problem and speed up the solution procedure, we find and exclude dominated routes. In general, if using one route always picks up the next cargo earlier at lower costs, this route dominates the other. However, when we introduce speed optimization, time and cost for using a route differ when using different speeds.

To establish dominance regarding the routes for repositioning for a given cargo pair i and j, we compare the earliest possible time cargo j can be picked up, T_{jr}^{min} when repositioning along route r, and the lowest and highest cost for repositioning along route r, C_{ijr}^{min} and C_{ijr}^{max}, respectively. We consider route r' to be dominated by route r if

$$T_{jr}^{min} \leq T_{jr'}^{min} \quad \text{and} \quad C_{jr}^{min} \leq C_{jr'}^{min} \quad \text{and} \quad C_{ijr}^{max} \leq C_{ijr'}^{max}.$$

These inequalities imply that route r is always as cheap as route r' while at the same time allowing an earlier pickup of cargo j. Route r' is therefore dominated and the corresponding decision variable for repositioning can be eliminated from the problem.

We require here that is possible to pick up cargo j within the given time window. We further assume that cargo i is picked up as early as possible, i.e. at time A_i. The time and cost parameters are then estimated as follows:

– *Estimating earliest possible pickup time,* T_{jr}^{min} The earliest possible pickup time is based on sailing as fast as possible after picking up cargo i to arrive at the pickup port of cargo j as early as possible. We define T_{jr}^{min} as follows:

$$T_{jr}^{min} = \max\{\text{arrival time when sailing as fast as possible}, A_j\}$$

This definition ensures that we do not pick up cargo j before its pickup time window opens, even if the vessel arrives earlier.

– *Estimating latest possible pickup time,* T_{jr}^{max} The latest possible pickup time is based on sailing as slow as possible after picking up cargo i while ensuring that we pick up cargo j within its time window. Unnecessary waiting after arriving at the pickup port is not allowed as this will only increase cost and delay departure. We define T_{jr}^{max} as follows:

$$T_{jr}^{max} = \max\{\min\{\text{arrival time when sailing as slow as possible}, B_j\}, A_j\}$$

The definition for T_{jr}^{max} is slightly more complicated to ensure that we always pickup the cargo within the time window. The inner minimum ensures that we never pick up cargo j after the time window closes, while the outer maximum ensures that we never pick up cargo j before the time window opens.

– *Estimating highest costs of repositioning along route* r, C_{ijr}^{max} The highest cost of repositioning along route r, C_{ijr}^{max}, is related to picking up cargo j as early as possible, i.e. at time T_{jr}^{min}. This is due to sailing at the highest necessary speed and therefore incurring higher fuel cost.

– *Estimating lowest costs of repositioning along route* r, C_{ijr}^{min} The lowest cost of repositioning along route r, C_{ijr}^{min}, is related to picking up cargo j as late as possible, i.e. at time T_{jr}^{max}. This is due to slow steaming reducing the fuel consumption, thus lowering the fuel cost but also postponing the arrival time.

5.4 Valid inequalities

Here we present the valid inequalities used to strengthen our formulation with regard to speed variables for delivery voyages. If waiting is inevitable for a repositioning voyage corresponding to variable x_{vijrs}, as described before the minimum speed will be chosen for the repositioning voyage. In addition, the delivery voyage for cargo i will also automatically select the minimum speed in the optimal solution. This observation leads to the following inequality:

$$\sum_{k \in \mathcal{K} | k \neq 1} y_{visk} + w_{vijrs1} \leq 1 \qquad x_{vijrs} \in X^{Wait}, \tag{20}$$

where X^{Wait} is the set of the repositioning variables where waiting is inevitable. Constraints (20) stipulate that if a repositioning voyage uses the minimum speed, then the corresponding delivery voyage will not use any other speed than the minimum speed as well. We refer to Constraints (20) as continuous inequalities.

With the dominance in repositioning speed variables and Constraints (13), the w variables can be replaced by the corresponding x variables, as only the minimum speed will be included in the optimal solution. Then we derive the alternative to Constraints (20), which we refer to as the binary inequalities as follows:

$$\sum_{k \in \mathcal{K} | k \neq 1} y_{visk} + x_{vijrs} \leq 1 \qquad x_{vijrs} \in X^{Wait}, \tag{21}$$

Table 1 Distances between ports

Distances (nm)	Yokohama	Busan	Singapore	Vladivostok	Hong Kong	Rotterdam	Antwerp	Bilbao
Yokohama	0	657	2892	937	1584	11,180	11,185	10,680
Busan	–	0	2503	509	1140	10,791	10,796	10,291
Singapore	–	–	0	3007	1460	8288	8293	7788
Vladivostok	–	–	–	0	1639	11,295	11,300	10,795
Hong Kong	–	–	–	–	0	9748	9753	9248
Rotterdam	**6885**	**7232**	**9697**	**6763**	**8334**	0	149	771
Antwep	**6980**	**7327**	**9792**	**6858**	**8429**	–	0	776
Bilbao	**7557**	**7904**	**10,369**	**7435**	**9006**	–	–	0

Distances of local and SCR voyages are at the higher triangle while distances for NSR voyages are in bold at the lower triangle

We test the performance with the original model in Sect. 4, including only Constraints (20) and including only Constraints (21). The results indicate that including Constraints (21) is the most effective formulation with regard to solution speed.

6 Input data and scenario generation

In this section we first introduce the input data for the case study with a 90-day planning horizon, then describe the scenario generation procedure. Please note that the input data for our study is not taken from a specific shipping company. Still, we use realistic and publicly available data either directly wherever possible or base our input data on such data.

6.1 Input data

Port information

We select eight ports among the busiest ports in Asia and Europe in the case study, including Yokohama, Busan, Singapore, Vladivostok, Hong Kong, Rotterdam, Antwerp and Bilbao. The distances between each port pair are listed in Table 1. We adopt the distances on sea-distances.org (2020) for local voyages and SCR voyages. For voyages through the NSR, we divide the voyage into three legs: from the European port to Murmansk, from Murmansk to Nome, and from Nome to the Asian port. We then add the lengths of the three legs together for an approximation.

Fleet

We include two types of vessels: open water and ice-going vessels, two of each type in the fleet. Vessels of the same type are identical except for their initial positions. The two types of vessels differ in fuel consumption profiles. We use the fuel consumption profile for a Handymax vessel of 40,000 DWT at selected speed alternatives. Consumption rate at design speed 13.5 kn is 0.1 ton/nm. At the maximum speed 15 kn, the consumption rate is 0.136 ton/nm and at the maximum speed 15 kn, 0.077 ton/nm. We adopt this data for the fuel consumption profile of open water vessels sailing fully loaded on SCR and local voyages.

Table 2 Fuel consumption rates for fully loaded vessels

Vessel type	Speed (kn)		Fuel consumption (ton/nm)
	SCR and local	NSR	
Open water	10.5	8.5	0.077
	13.5	11.5	0.1
	15	13	0.136
Ice-going	10.5	9.5	0.084
	13.5	12.5	0.109
	15	14	0.148

When sailing along the NSR, due to the presence of sea ice, the speed of open water vessels reduces by 2 kn. For an ice-going vessel, we follow the assumption in Lasserre (2014) that it consumes 9% more fuel than the open water vessel at the same speed. Similarly, ice-going vessels receive 1 kn speed reduction when sailing on NSR. The fuel consumption rates for fully loaded vessels of both types are summarized in Table 2. According to Gkonis and Psaraftis (2012), the consumption rate sailing in ballast is about 80% of the corresponding rate of sailing fully loaded.

Costs

The voyage cost consists of fuel cost, port due and transit fee if it is intercontinental. We set the fuel price to 175.5 USD/mt, the average of Europe, the Middle East and Africa (EMEA) and Asia-Pacific fuel prices as of April 2020. We adopt the port dues in Zhu et al. (2018), 23,200 USD per voyage. The transit fee is based on Suez Canal Authority (2017) for SCR and The Northern Sea Route Administration (2019) for NSR, including ice-breaking support fees.

According to Brouer et al. (2014), the daily fuel consumption while being idle can be approximated to be 10% of the fuel consumption while sailing at the design speed. We follow this assumption when calculating the idle fuel cost as well as the CO_2 emissions.

CO_2 emissions and carbon tax

According to International Maritime Organization (2009), each ton of Heavy Fuel Oil emits 3.114 tons CO_2. With this factor, we convert the total fuel consumption for the fleet into the total CO_2 emissions.

We consider two carbon tax schemes. The Norwegian Government (2019) sets the carbon tax to be 60 USD per ton CO_2 for the shipping industry. We adopt this tax rate in a flat carbon tax scheme. In the progressive tax scheme, we estimate the tax rate and the emission levels as shown in Table 3. The emission levels are estimated considering the total emissions for the fleet in the planning horizon.

6.2 Scenario generation

We create scenario trees containing cargo information for the case study. All scenario trees share the same 15 deterministic cargoes and initial location cargo of each vessel. Each scenario

Table 3 Carbon tax rates in progressive tax scheme

CO_2 emissions (ton)	Carbon tax rate (USD/ton)
0–7000	40
7000–14,000	60
14,000–21,000	80
> 21,000	100

contains in addition up to 35 scenario-dependent available spot cargoes. We summarize the procedure to generate scenarios below:

1. *Cargo Pool Generation* We first create a candidate cargo pool consisting of 1000 cargoes. For each cargo, we generate the pickup and delivery ports, pickup time window and revenue rate. Among the 1000 candidate cargoes, 700 are intercontinental, while the remaining 300 are divided equally into European and Asian local cargoes. For intercontinental cargoes, we randomly select a pickup port from the eight available ports. We then sample the delivery port from the remaining ports on the other continent. Pickup time for each cargo is sampled randomly from the planning horizon. For local cargoes we use a similar procedure except that the delivery port is sampled from the remaining ports on the same continent. The time window for picking up the cargo is set to either three or seven days. The freight rate for each cargo follows a uniform distribution between 175% to 200% of the total costs of transporting the cargo with a lower ice-class vessel at design speed either locally or via SCR. To initialize the problem and to ensure that all vessels can end their voyages in any port, we define artificial origin and destination cargoes for each vessel with a freight rate of 0. The origin cargo is to be delivered at the port where the vessel is first becoming available during the planning horizon. The destination cargo can be picked up and delivered throughout the entire planning horizon as a vessel's last cargo. Pickup and delivery for the destination cargo is set to an artificial port with no repositioning time or cost to any other port.
2. *Sampling Deterministic Cargoes* The probability of a cargo being chosen as a deterministic cargo follows a triangular distribution based on the earliest pickup time of the cargo. We assume that cargoes with an early pickup time have a higher probability of being deterministic, while cargoes becoming available at the end of the planning horizon have a lower probability of being deterministic cargoes. This assumption reflects that typically more information is available for the near future. After assigning the probabilities, we sample the deterministic cargoes as follows: We first draw a cargo (with all cargoes being equally likely) and then sample if this cargo will be included as a deterministic cargo. If the cargo is included, it is removed from the candidate pool and we stop once 15 deterministic cargoes have been included.
3. *Sampling Available Spot Cargoes* Here we sample 35 spot cargoes with equal probability from the remaining 985 cargoes for each scenario. For each spot cargo, the probability for it to be available in a given scenario is set to 50%. We only include available spot cargoes in the different scenarios.

Note that we use Monte Carlo sampling and uniform distributions to generate the candidate pool of cargoes. When generating a scenario tree, we first use Monte Carlo sampling to select the cargoes and then sample based on the specified distributions to determine whether or not to include a cargo in the tree. However, our approach is not limited to this sampling procedure and can easily be adapted if more realistic data is available.

Table 4 Settings for different cases

Case	Speed optimization	Carbon tax scheme
Basic	Design speed	No tax
Tax	Design speed	Flat tax
Speed	Speed optimization	No tax
Flat	Speed optimization	Flat tax
Prog	Speed optimization	Progressive tax

7 Case study

We create five cases for our case study. In each case, we create an instance (SCR+NSR) where we allow both SCR and NSR and a reference instance (SCR) where we allow only the SCR. All five cases share the same scenario trees but they differ in whether we allow speed optimization and the carbon tax schemes. The settings of the different cases are listed in Table 4. In the basic case (Basic), we include neither speed optimization nor carbon tax. We then solve a case where we include a flat carbon tax but no speed optimization (Tax). These two cases use design speed only. We have one case including speed optimization but no carbon tax (Speed). We also combine speed optimization with a flat carbon tax (Flat) and a progressive carbon tax (Prog).

7.1 Solutions

As we cannot solve our two-stage stochastic programming problem directly, we use Sample Average Approximation (SAA) to find good solutions for our problem (see Kleywegt et al. 2002 e.g., for details). As part of the SAA approach, we solve 60 two-stage stochastic programming problems with 10 scenarios each. The average of the resulting objective function values serves as a statistical upper bound for the true objective function value. To find a lower bound for the true objective function value, we evaluate the first-stage solutions found in these problems in a reference sample of 1000 scenarios. This reference sample represents the uncertainty in the original problem. For a more detailed description of the SAA approach, we refer to Schütz et al. (2009).

We implement and solve the problems using FICO Xpress 8.10. We carry out all computations on Lenovo NextScale nx360 M5 computers with two 3.4 GHz Intel 6-core E5-2643 CPUs and 512 GB RAM running a Linux operating system. For each problem, we limit the maximum run time to one hour and stop earlier if the optimality gap falls below 0.01%. In Table 5, we summarize the results from solving 60 problems for each instance. In particular, we report how many of the problems have not been solved to optimality, the average optimality gap over all 60 problems and the worst optimality gap.

The problems for the Basic and Tax cases are all solved to optimality within the time limit. The other three cases with speed optimization (Speed, Flat, and Prog) are slightly more difficult to solve, with SCR+NSR being harder than SCR. Introducing a carbon tax adds to the complexity of the problem. All problems from the reference sample are solved to optimality.

Table 6 summarizes the solutions for the different cases. The optimality gaps for the different cases are estimated based on the upper and lower bounds found using SAA. For the cases where not all problems are solved to optimality, we use the upper bounds from the 60 problems to calculate the estimator of the upper bound for the true problem. We see that

Table 5 Properties of the 60 problems for each instance

Case	Instance	Non optimal	Average optimality gap (%)	Worst optimality gap (%)
Base	SCR	0	0	0.01
	SCR+NSR	0	0	0.01
Tax	SCR	0	0	0.01
	SCR+NSR	0	0	0.01
Speed	SCR	7	0.13	2.70
	SCR+NSR	35	0.37	3.69
Flat	SCR	17	0.50	4.28
	SCR+NSR	38	0.64	3.93
Prog	SCR	17	0.58	3.99
	SCR+NSR	36	0.82	3.80

Table 6 Solution quality of the different cases

Case	Instance	Estimated optimality gap (%)	Lower bound	Upper bound
Base	SCR	1.62	597.09	606.90
	SCR+NSR	3.29	734.27	759.24
Tax	SCR	1.37	427.13	433.07
	SCR+NSR	2.62	592.94	608.87
Speed	SCR	4.21	625.89	653.39
	SCR+NSR	2.18	823.19	841.50
Flat	SCR	3.36	476.67	493.23
	SCR+NSR	2.43	680.45	697.38
Prog	SCR	2.99	464.58	478.92
	SCR+NSR	2.69	673.99	692.59

the estimated optimality gaps for the different cases are within 3.5%, with one case being as large as 4.21%. These solutions are considered good enough for practical purposes.

We notice that in the Basic and Tax cases, the estimated optimality gaps from the SCR instances are smaller than the SCR+NSR instances. But for the cases with speed optimization, the estimated optimality gaps from the SCR+NSR instances are smaller. Compared to the SCR instances, the solution space in the SCR+NSR instances is larger, resulting in higher bounds for all SCR+NSR instances. When we look at the speed optimization cases for the SCR instances, we utilize only the variable reduction related to speed, but no dominance for repositioning. As for SCR+NSR instances, we utilize both speed variable reduction and routing variable reduction. It is possible that the combined pre-processing procedure outperforms the individual ones. Another possible explanation of the smaller gaps for the SCR+NSR instances with speed optimization is that introducing the NSR is even more beneficial. This might help in cutting off large parts of the branch and bound tree early in the solution process.

Table 7 Costs and revenues in million USD in the best solutions

Case	Instance	Cargo revenues	Delivery costs	Repositioning costs	Idle costs	Carbon tax	Gross margin
Base	SCR only	9.49	2.89	0.59	0.03	0.00	5.97
	SCR+NSR	10.55	2.61	0.55	0.05	0.00	7.34
Tax	SCR only	9.05	2.77	0.31	0.05	1.65	4.27
	SCR+NSR	10.33	2.58	0.39	0.06	1.37	5.93
Speed	SCR only	9.32	2.69	0.34	0.03	0.00	6.26
	SCR+NSR	11.61	2.75	0.61	0.02	0.00	8.23
Flat	SCR only	9.20	2.63	0.30	0.03	1.47	4.77
	SCR+NSR	11.33	2.65	0.48	0.02	1.37	6.80
Prog	SCR only	9.11	2.58	0.30	0.03	1.55	4.65
	SCR+NSR	11.22	2.61	0.47	0.02	1.38	6.74

7.2 Impact of the NSR

7.2.1 Economic impact

We present the costs and revenues of the best solutions for the different cases in Table 7. When allowing NSR, the gross margins always exceed the gross margins compared to SCR only. Among all costs, delivery costs have the largest share, followed by carbon tax (if applicable) and repositioning costs. Idle costs only represent a marginal share of the total costs. Using the NSR always results in higher cargo revenues compared only using SCR. However, the delivery costs increase only slightly (Speed, Flat, Prog) or even decrease (Base, Tax). These results indicate using the NSR benefits the tramp operators economically.

The Tax case gives the least profits across all the presented cases. However, introducing carbon tax amplifies the advantage of using the NSR. For the SCR instances, compared with the non-tax counterparts, we find a decrease in cargo revenues and almost all costs, causing a decrease in gross margin. The same pattern applies to the SCR+NSR instances as well. Comparing the profits of the three cases with carbon tax to their no tax counterparts, we find using the NSR is more robust than using only the SCR. For SCR only instance for example, the gross margin is reduced by 1.70 million USD from the Base case to the Tax case. In the corresponding SCR+NSR instances, the gross margin is reduced by only 1.41 million. We see a similar effect for also speed optimization, albeit less pronounced for the flat carbon tax, but more pronounced for the progressive carbon tax. It is also worth mentioning that in the cases with carbon tax (Tax, Flat, Prog), the SCR+NSR instances result in both higher cargo revenues and lower carbon taxes.

Compared to the Base and Tax cases, both of their speed optimization counterparts have a higher gross margin as well as lower idle costs and carbon tax. This indicates that speed optimization is a viable approach for tramp operators to cope with the carbon tax and improve fleet utilization. We observe different impacts of speed optimization in the SCR instances and the SCR+NSR instances. In the SCR instances, we see a reduction in delivery costs and repositioning costs, with minor deviations in cargo revenues. But the gross margins overall increase. The increased gross margin comes mainly from reduced costs. In contrast, cargo revenues increase significantly when allowing speed optimization in SCR+NSR instances, with slight increase in delivery and repositioning costs. The gross margin increases mainly due to increased cargo revenues. It is also worth mentioning that in the speed optimization

Table 8 Average number of voyages in the best solutions

Case	Instance	Delivery voyages					Repositioning voyages				
		SCR	NSR	European	Asian	Sum	SCR	NSR	European	Asian	None
Base	SCR only	7.01	0.00	2.35	2.58	11.94	0.99	0.00	3.08	3.51	4.35
	SCR+NSR	0.94	6.70	1.64	2.53	11.81	0.37	0.69	2.20	4.12	4.43
Tax	SCR only	6.91	0.00	1.31	1.96	10.19	0.41	0.00	1.68	3.18	4.92
	SCR+NSR	0.75	6.94	1.38	1.44	10.51	0.05	0.68	1.89	3.01	4.88
Speed	SCR only	6.93	0.00	1.19	2.14	10.26	0.52	0.00	1.73	3.36	4.66
	SCR+NSR	1.25	7.30	1.29	2.37	12.21	0.22	1.07	2.02	4.44	4.46
Flat	SCR only	6.91	0.00	0.86	1.86	9.63	0.48	0.00	1.48	3.21	4.46
	SCR+NSR	0.92	7.59	0.94	1.17	10.62	0.08	1.11	1.70	3.14	4.60
Prog	SCR only	6.86	0.00	0.76	1.75	9.37	0.50	0.00	1.38	3.12	4.38
	SCR+NSR	0.84	7.60	0.80	1.08	10.32	0.06	1.12	1.60	3.05	4.49

cases, less idle costs are paid in the SCR+NSR instances than in the SCR only instances. The results indicate that the fleet utilization increases when using speed optimization.

To further investigate the impact of the NSR on tramp shipping routing decisions, we look into the number of delivery and repositioning voyages by region, see Table 8. In the following, we examine the effects of the introduction of a carbon tax. Introducing a carbon tax causes a reduction in total cargoes transported in all cases. This finding is in line with the decrease in revenues that we have discussed previously. With the exception of the Base case, we see that fewer cargoes are transported across regions in the SCR instances. For the SCR+NSR instances, we see an increase in number of cargoes and a shift towards sailing along the NSR. Specifically, the number of transported intercontinental cargoes increases compared to the SCR instances. Such a pattern is reasonable, as intercontinental cargoes in general bring more revenue compared to the local cargoes. These findings also support that when carbon tax imposed, the advantage of using the NSR is amplified.

When introducing speed optimization in the SCR instances, the number of transported cargoes is reduced. However, the idle costs do not go up, implying idle time does not increase. It is very likely that slow steaming is used in these instances and hence the costs are reduced. For the SCR+NSR instances, we see an increase in both the number of intercontinental SCR and NSR cargoes, with fewer local cargoes being transported. With the routing flexibility introduced by NSR, speed optimization allows for transporting more cargoes, or cargoes with higher revenues.

In terms of repositioning choices, the most popular choice is to go without repositioning, meaning that after delivering a cargo, the vessel waits at the same port to pick up its next cargo. Local repositioning is more favored than intercontinental repositioning. This is reasonable as the time spent on repositioning only adds to the cost. Long intercontinental repositioning is therefore least favorable. This also explains why the NSR is much more used for intercontinental repositioning. Similar repositioning patterns are found in Li et al. (2020).

7.2.2 Average speeds and CO_2 emissions

We calculate the average speeds by vessel types and regions. Since fuel consumption profiles are identical for the same vessel along the SCR and local voyages, we combine them in the

Table 9 Average speeds and CO_2 emissions

Case	Instance	Open water vessels speed (kn)		Ice-going vessels speed (kn)		CO_2 emissions (tons)
		SCR+local	NSR	SCR+local	NSR	
Base	SCR only	13.5	–	13.5	–	30617
	SCR+NSR	13.5	11.5	13.5	12.5	25084
Tax	SCR only	13.5	–	13.5	–	27455
	SCR+NSR	13.5	11.5	13.5	12.5	22860
Speed	SCR only	12.89	–	12.80	–	25574
	SCR+NSR	12.18	10.15	13.09	11.28	25110
Flat	SCR only	12.85	–	12.72	–	24493
	SCR+NSR	11.71	9.66	13.01	11.12	22737
Prog	SCR only	12.88	–	12.71	–	23917
	SCR+NSR	11.57	9.53	13.21	11.02	22136

following presentation. Table 9 summarizes the average speed for all delivery and repositioning voyages for each vessel type in each region. In addition, the table also shows the CO_2 emissions. Please note that the Base and Tax case use constant design speed.

When speed optimization is allowed, carbon taxes generally lead to lower average speeds. Compared to the Speed case however, the speed of ice-going vessels in SCR and local voyages actually increases in the Prog case. A closer examination into the usage of ice-going vessels indicates that this increase comes from an increase in repositioning speed within Europe, which might be due to the pickup time window limitation. It is worth mentioning that the extent of speed reduction affected by carbon tax differs for the two types of vessels. Open-water vessels generally decrease their speed more than ice-going vessels. In general, the average speeds are always below the design speeds. This behavior confirms the prevailing practice of slow steaming.

In terms of reducing CO_2 emissions, carbon taxes are effective in reducing the total volume, in both the SCR instances and the SCR+NSR instances. Without speed optimization, CO_2 emissions are reduced by approximately 10%. With speed optimization, the reduction in CO_2 emissions is less at around 4–6%. Using the NSR generally reduces CO_2 emissions due to lower speeds, despite an increase in the number of transported cargoes, indicating that using the NSR can be a viable approach to cope with the decarbonization goal.

8 Conclusion

We present a new variant of stochastic TSRSP with speed optimization and carbon tax. We formulate it as a two-stage stochastic programming model where we model the speed optimization through a piece-wise linear approximation. Our model also allows for flexibility in using the SCR or NSR for intercontinental voyages. We evaluate the impact of the NSR on tramp shipping, in terms of gross margins and CO_2 emissions considering speed optimization and carbon tax.

The results from case study show that introducing the NSR improves the gross margins and can reduce the CO_2 emissions for tramp operators. The carbon tax is effective in reducing the CO_2 emissions, but it reduces the gross margins as well. Note that our analysis focuses

on full shiploads and it will be interesting to study the effects of the carbon tax on tramp shipping with partial shiploads. In any case, to take full advantage of the carbon tax, it should be combined with CO_2 compensation.

We also see an increase in the number of intercontinental voyages when the NSR introduced. The NSR is more preferred over the SCR and when we impose a carbon tax, the advantage of using the NSR is amplified. Using the NSR with speed optimization allows for transporting more cargoes while maintaining low CO_2 emissions. The impact of using synthetic fuels, in particular low- and zero-emission fuels such as ammonia and hydrogen, should be investigated in more detail.

Note that increasing shipping activities along the NSR may influence local climate change and increase the melting of sea ice. However, these effects are outside the scope of this paper and subject to future research.

Funding Open access funding provided by NTNU Norwegian University of Science and Technology (incl St. Olavs Hospital - Trondheim University Hospital)

References

Andersson, H., Fagerholt, K., & Hobbesland, K. (2015). Integrated maritime fleet deployment and speed optimization: Case study from roro shipping. *Computers & Operations Research, 55*, 233–240.

Brouer, B. D., Alvarez, J. F., Plum, C. E., Pisinger, D., & Sigurd, M. M. (2014). A base integer programming model and benchmark suite for liner-shipping network design. *Transportation Science, 48*(2), 281–312.

Castillo-Villar, K. K., González-Ramírez, R. G., Miranda González, P., & Smith, N. R. (2014). A heuristic procedure for a ship routing and scheduling problem with variable speed and discretized time windows. *Mathematical Problems in Engineering* (2014).

Christiansen, M., & Fagerholt, K. (2014). Ship routing and scheduling in industrial and tramp shipping. In P. Toth & D. Vigo (Eds.), *Vehicle routing: Problems, methods, and applications* (2nd ed., pp. 381–408). SIAM—Society for Industrial and Applied Mathematics.

Christiansen, M., Fagerholt, K., Nygreen, B., & Ronen, D. (2007). Maritime transportation. *Handbooks in Operations Research and Management Science, 14*, 189–284.

Gkonis, K. G., & Psaraftis, H. N. (2012). Modeling tankers' optimal speed and emissions. *Society of Naval Architects and Marine Engineers Transactions, 120*, 90–115.

International Maritime Organization. (2009). *Guidelines for voluntary use of the ship energy efficiency operational indicator (EEOI)*. IMO. Retrieved January 7, 2021, from https://wwwcdn.imo.org/localresources/en/OurWork/Environment/Documents/Circ-684.pdf

International Maritime Organization. (2020). *Reduction of GHG emissions from ships: Fourth IMO GHG study 2020 - final report*. IMO. Retrieved January 7, 2021, from https://imoarcticsummit.org/wp-content/uploads/2020/09/MEPC-75-7-15-Fourth-IMO-GHG-Study-2020-Final-report-Secretariat.pdf

Kleywegt, A. J., Shapiro, A., & Homem-de Mello, T. (2002). The sample average approximation method for stochastic discrete optimization. *SIAM Journal on Optimization, 12*(2), 479–502.

Lasserre, F. (2014). Case studies of shipping along Arctic routes. Analysis and profitability perspectives for the container sector. *Transportation Research Part A: Policy and Practice, 66*, 144–161.

Li, M., Fagerholt, K., & Schütz, P. (2020). Analyzing the impact of the Northern Sea Route on tramp ship routing with uncertain cargo availability. In E. Lalla-Ruiz, M. Mes, & S. Voß (Eds.), *Lecture Notes in Computer Science* (Vol. 12433, pp. 68–83). Springer.

Meng, Q., Zhang, Y., & Xu, M. (2017). Viability of transarctic shipping routes: A literature review from the navigational and commercial perspectives. *Maritime Policy & Management, 44*(1), 16–41.
Milaković, A. S., Gunnarsson, B., Balmasov, S., Hong, S., Kim, K., Schütz, P., & Ehlers, S. (2018). Current status and future operational models for transit shipping along the Northern Sea Route. *Marine Policy, 94*, 53–60.
Norstad, I., Fagerholt, K., & Laporte, G. (2011). Tramp ship routing and scheduling with speed optimization. *Transportation Research Part C: Emerging Technologies, 19*(5), 853–865.
Pierre, C., & Olivier, F. (2015). Relevance of the Northern Sea Route (NSR) for bulk shipping. *Transportation Research Part A: Policy and Practice, 78*, 337–346.
Ronen, D. (1982). The effect of oil price on the optimal speed of ships. *Journal of the Operational Research Society, 33*(11), 1035–1040.
Schøyen, H., & Bråthen, S. (2011). The Northern Sea Route versus the Suez Canal: Cases from bulk shipping. *Journal of Transport Geography, 19*(4), 977–983.
Schütz, P., Tomasgard, A., & Ahmed, S. (2009). Supply chain design under uncertainty using sample average approximation and dual decomposition. *European Journal of Operational Research, 199*(2), 409–419.
sea-distances.org (2020). *Sea Distances/Port Distances*. Retrieved April 2, 2019, from https://sea-distances.org/
Suez Canal Authority. (2017). *Tolls calculator. Suez Canal Authority*. Retrieved April 2, 2019, from https://www.suezcanal.gov.eg/English/Tolls/Pages/TollsCalculator.aspx
The Northern Sea Route Administration. (2019). *Icebreaker assistance value calculating. The Northern Sea Route Administration*. Retrieved April 2, 2019, from http://www.nsra.ru/en/ledokolnaya_i_ledovaya_lotsmanskaya_provodka/raschet_stoimosti_ledokolnoy_provodki_v_akvatorii_smp.html
The Norwegian Government. (2019). *The government's action plan for green shipping. The Norwegian Government*. Retrieved January 2, 2021, from https://www.regjeringen.no/en/dokumenter/the-governments-action-plan-for-green-shipping/id2660877/
Theocharis, D., Pettit, S., Rodrigues, V. S., & Haider, J. (2018). Arctic shipping: A systematic literature review of comparative studies. *Journal of Transport Geography, 69*, 112–128.
Tirado, G., Hvattum, L. M., Fagerholt, K., & Cordeau, J. F. (2013). Heuristics for dynamic and stochastic routing in industrial shipping. *Computers & Operations Research, 40*(1), 253–263.
United Nations Conference on Trade and Development. (2020). *Review of Maritime Transport 2020. United Nations Conference on Trade and Development*. Retrieved January 2, 2021, from https://unctad.org/system/files/official-document/rmt2020_en.pdf
Vilhelmsen, C., Larsen, J., & Lusby, R. M. (2015). *Tramp ship routing and scheduling - models, methods and opportunities*. DTU Management Engineering. Technical University of Denmark.
Wang, X., Norstad, I., Fagerholt, K., & Christiansen, M. (2019). Green tramp shipping routing and scheduling: Effects of market-based measures on CO_2 reduction. In H. N. Psaraftis (Ed.), *Sustainable Shipping* (pp. 285–305). Springer.
Wen, M., Ropke, S., Petersen, H. L., Larsen, R., & Madsen, O. B. (2016). Full-shipload tramp ship routing and scheduling with variable speeds. *Computers & Operations Research, 70*, 1–8.
Wen, M., Pacino, D., Kontovas, C., & Psaraftis, H. (2017). A multiple ship routing and speed optimization problem under time, cost and environmental objectives. *Transportation Research Part D: Transport and Environment, 52*, 303–321.
Wu, L., Pan, K., Wang, S., & Yang, D. (2018). Bulk ship scheduling in industrial shipping with stochastic backhaul canvassing demand. *Transportation Research Part B: Methodological, 117*, 117–136.
Yu, B., Peng, Z., Tian, Z., & Yao, B. (2019). Sailing speed optimization for tramp ships with fuzzy time window. *Flexible Services and Manufacturing Journal, 31*(2), 308–330.
Zhang, Z., & Baranzini, A. (2004). What do we know about carbon taxes? An inquiry into their impacts on competitiveness and distribution of income. *Energy Policy, 32*(4), 507–518.
Zhao, H., & Hu, H. (2016). Study on economic evaluation of the Northern Sea Route: Taking the voyage of Yong Sheng as an example. *Transportation Research Record, 2549*(1), 78–85.
Zhu, S., Fu, X., Ng, A. K., Luo, M., & Ge, Y. E. (2018). The environmental costs and economic implications of container shipping on the Northern Sea Route. *Maritime Policy & Management, 45*(4), 456–477.